DOI: 10.1017/S1431927605507530

Microsc Microanal 11(Suppl 2), 2005

Cross-fringe versus single-fringe probabilities

W. Qin[1], P. Fraundorf[2]

[1] Advanced Products R&D Lab, Freescale Semiconductor, Inc., MD CH305, 1300 N. Alma School Road, Chandler, AZ 85224
[2] Department of Physics and Astronomy and Center for Molecular Electronics, University of Missouri-St. Louis, St. Louis, MO 63121

High-resolution TEM is well-suited to characterizing nanocrystals, where lattice fringes serve as a source of structural information [1, 2]. Based on 2D lattice fringe images taken at different specimen orientations, 3D lattice parameters can be determined [3-6]. Recent work has shown that lattice fringe-visibility maps, a thin-specimen extension of bend-contour and channeling-pattern maps, can assist crystallographic study in direct space much as do Kikuchi maps in reciprocal space [7]. A nanocrystal can be tilted while the condition for visualizing a set of lattice fringes is maintained so as to "acquire" new lattice fringe normals (co-vectors), and thus continually refine a basis triplet containing information on both the nanocrystal's lattice and its orientation. Local specimen thickness measurements are another promising possibility.

Probabilities inferred from fringe-visibility maps further allow one to quantify the abundance of fringes in collections of randomly-oriented nanoparticles. In the thin-specimen limit, a fringe-visibility band has a band-width proportional to d/t, rather than the λ/d proportionality expected for large t, where d is the lattice spacing, t is specimen thickness, and λ is electron wavelength. This follows from the expression for bandwidth half-angle at arbitrary thickness:

$$\alpha_{\max} = \sin^{-1}\left[\frac{df}{t} + \frac{\lambda}{2d}\left(1 - \left(\frac{df}{t}\right)^2\right)\right], \tag{1}$$

where f is a "visibility factor" on the order of 1 that empirically accounts for signal-to-noise in the method used to detect fringes [7]. The first term in (1) dominates for $t < 2\, d^2\, f/\lambda$ and therefore in typical TEMs for inter-atom spacings in particles 10 nm in size and smaller.

Fig. 1 shows the {200}, {111} and {220} fringe-visibility bands of a spherical f.c.c. nanocrystal. The probability of the (hkl) lattice plane to show is therefore that fraction of the solid angle subtended by the corresponding visibility band, i.e. $p_{(hkl)} = \sin[\alpha_{\max}] \cong d_{hkl}f/t$ in the thin-specimen limit. Band intersections correspond to regions of visible cross-fringes. Calculation of the area of an intersection between visibility bands [7] indicates that flat-polygon intersection areas are an excellent small-angle approximation, in some cases with errors on the order of $\alpha_{\max}^6$. With this approximation, the probability of cross-fringes from lattice planes 1 and 2, whose fringe-visibility bands have half-widths α_1 and α_2 and intersect at an angle of ϕ, is $p_{1\times 2} = 2\alpha_1\alpha_2/(\pi \sin\phi)$.

Figure 2 illustrates the fraction of randomly-oriented fcc particles showing only un-crossed (111) fringes, and that showing <110> zone cross-fringes. It is obvious that cross-fringe grains become more abundant than single-fringe grains as the grain diameter t decreases below 3 nm. This is because the zone area increases as $(df/t)^2$ while the single-fringe region increases as (df/t) and decrease in length at the expense of the zones. This model suggests, moreover, that the crossover size is quite sensitive to the visibility factor f for a given microscope/specimen combination. In such a small size range, though, the broadening of reciprocal spots warrants caution, as deceptive lattice fringes that are "Moires" instead of direct representations of the lattice planes may be formed, as a result of the low-pass filtering of projected potentials by the microscope [2]. Figures 3 and 4 show how zone axis areas (overlaps of bands) change as smaller spacings become reliably visible.

References:

1. S.-C.Y. Tsen, P. A. Crozier, J. Liu, Ultramicroscopy **98**(2003)63-72.
2. J. O. Malm, M. O'keefe, Ultramicroscopy **68**(1997)13.
3. P. Fraundorf, Ultramicroscopy **22**(1987)225
4. P. Möck, *Cryst. Res. Technol.* **26,** 653-658 (1991).
5. W. Qin and P. Fraundorf, Ultramicroscopy **94**(2003)245-262
6. W. Qin, Ph. D. Thesis, UM-StL/Rolla, 2000
7. P. Fraundorf et al., Making sense of nanocrystal lattice fringes, arXiv:cond-mat/0212281 (2005).

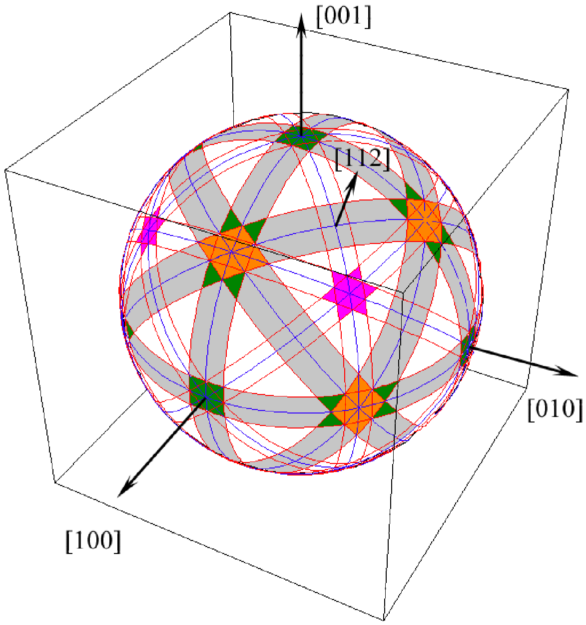

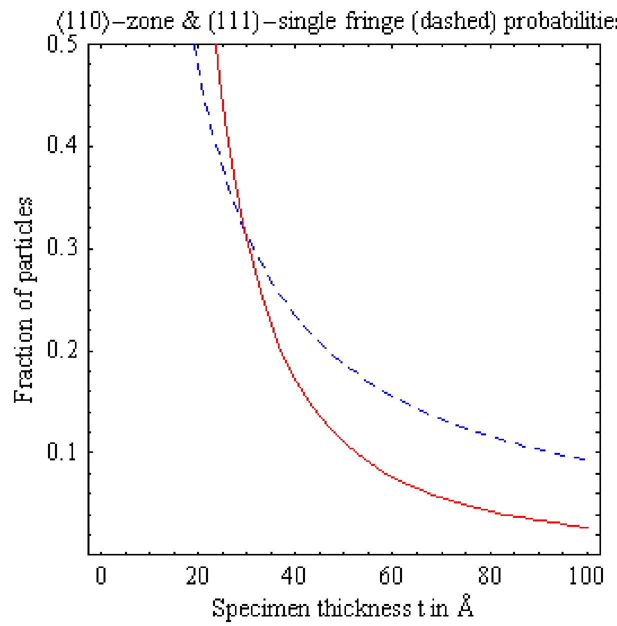

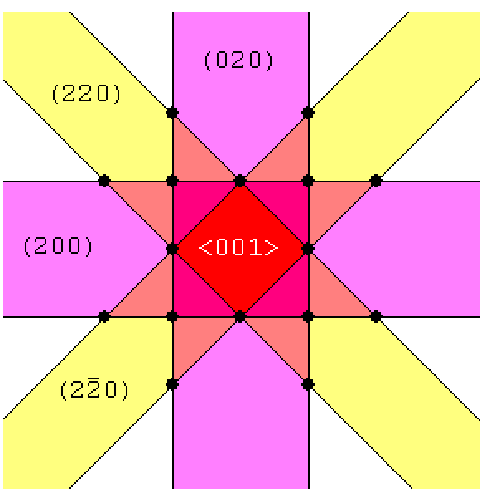

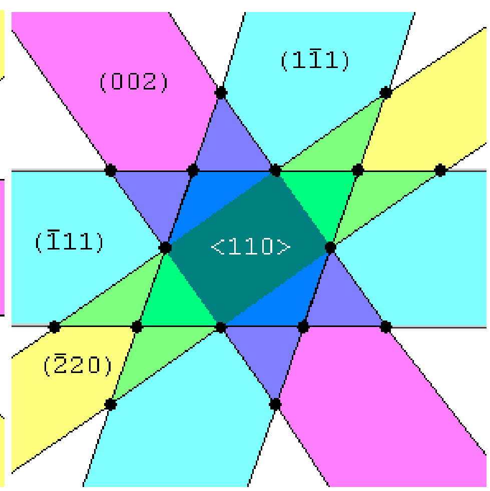

Figure 1 (upper left): The {200}, {111} (both shaded) and {220} (not shaded) fringe-visibility bands of a spherical f.c.c. nanocrystal.
Figure 2 (upper right): The reversal in relative abundance for cross-fringe versus single-fringe particles as a function of particle diameter.
Figure 3 (lower left): Polygonal cross-fringe zones for fcc ⟨001⟩ in the thin-specimen/small-angle approximations, built up as first {200} and then {220} fringes become visible.
Figure 4 (lower right). Polygonal cross-fringe zones for fcc ⟨110⟩ in the thin-specimen/small-angle approximations.

https://doi.org/10.1017/S1431927605507530 Published online by Cambridge University Press